Original

Georgopanos, P.; Lo, T.-Y.; Ho, R.-M.; Avgeropoulos, A.:

Synthesis, molecular characterization and self-assembly of (PS-b-PDMS)n type linear (n = 1, 2) and star (n = 3, 4) block copolymers

In: Polymer Chemistry (2016) Royal Society of Chemistry

DOI: 10.1039/C6PY01768A

Polymer Chemistry

PAPER

View Article Online
View Journal

Cite this: DOI: 10.1039/c6py01768a

Synthesis, molecular characterization and self-assembly of (PS-*b*-PDMS)$_n$ type linear (n = 1, 2) and star (n = 3, 4) block copolymers†

Prokopios Georgopanos,[a,b,c] Ting-Ya Lo,[c] Rong-Ming Ho*[c] and Apostolos Avgeropoulos*[a]

Received 10th October 2016,
Accepted 22nd November 2016

DOI: 10.1039/c6py01768a

www.rsc.org/polymers

Well-defined linear (n = 1, 2) and star (n = 3, 4) architecture [polystyrene-*b*-poly(dimethylsiloxane)]$_n$ or (PS-*b*-PDMS)$_n$ block copolymers were synthesized by anionic polymerization and using various chlorosilanes as linking agents. The self-assembly of the novel synthesized copolymers revealed that microphase separation for the star-block copolymers is significantly influenced by entropy constraints due to the increased number of junction points.

Introduction

The synthesis of polystyrene-*b*-poly(dimethylsiloxane) (PS-*b*-PDMS) diblock copolymers through ionic polymerization[1,2] has been examined since the early 70s[3,4] due to the unique properties of the semi-organic PDMS domains. The resistance of the PDMS blocks to a variety of etching techniques and, in particular, to UV radiation[5] leads to applicable cylindrical and lamellar nanostructures in bulk and thin films for nanotechnology applications such as nanolithography.[6] The effect of a complex architecture in microphase separation has been reported for various types of linear, star, star-block and miktoarm star copolymers.[7–14] To study the effect of an additional number of diblock arms on the topology and solution properties of the final material, when compared to the initial linear diblock copolymer, the synthesis of star-block copolymers of the (A-*b*-B)$_n$ type has been suggested,[15] where A and B are immiscible and strongly segregated blocks. Validation of the experimental data was accomplished also by theoretical approaches in both simple (diblock) and more complex (star-block) copolymers.[16–26] Other star-like polymers prepared by living radical polymerization have also been reported but they lack the homogeneity and the control of the final architecture when compared to similar polymers synthesized by anionic polymerization and combination of chlorosilane chemistry.[27,28] Matyjaszewski and co-workers synthesized star-block copolymers *via* atom transfer radical polymerization through the "core first",[29] the "arm first" methods[29,30] and their combinations by involving click chemistry for the linking of the arms.[31,32] Recently, the Avgeropoulos group reported the synthesis of [polystyrene-*b*-poly(2-vinylpyridine)]$_3$ or (PS-*b*-P2VP)$_3$ star-block copolymers *via* atom transfer radical polymerization and studies on the microphase separation in bulk led to well-defined morphologies in the absence of any catalyst residues.[33]

In this study, we report the synthesis of a series of linear (n = 1, 2) and star-block copolymers (n = 3, 4) of the (PS-*b*-PDMS)$_n$ type consisting of PS-*b*-PDMS diblock copolymer arms *via* chlorosilane chemistry. Their molecular/compositional homogeneity was verified through various characterization methods and we also studied their self-assembly in bulk. The synthesis of star block copolymers of the (PS-*b*-PDMS)$_3$ and (PS-*b*-PDMS)$_4$ types is novel and led to the formation of copolymers with the flexible blocks (PDMS) as the inner chains while the more stiff blocks (PS) are the outer chains. Additionally, by taking advantage of the strongly segregated character of the PS-*b*-PDMS copolymer, the architecture effect on the self-assembly is examined. Although the diblock copolymer precursors exhibit expected morphologies, a chevron texture was identified during the self-assembly of a (PS-*b*-PDMS)$_3$ type star-block copolymer. Such a chevron texture has been observed in the cases of rod-coil polymers,[34] semi-crystalline polymers[35] or mechanically stretched materials.[36–38] This unusual structure could be initially described as a structural defect similar to chevron defects identified in lamellar textures.[20,39] Also, such a topography has been observed for linear diblock copolymers of polystyrene-*b*-poly(butadiene) by Gido and co-workers.[40,41]

[a]*Department of Materials Science Engineering, University of Ioannina, University Campus – Dourouti, Ioannina 45110, Greece. E-mail: aavger@cc.uoi.gr*
[b]*Institute of Polymer Research, Helmholtz-Zentrum Geesthacht, Max-Planck-Str. 1, Geesthacht 21502, Germany*
[c]*Department of Chemical Engineering, National Tsing Hua University, Hsinchu 30013, Taiwan, Republic of China. E-mail: rmho@mx.nthu.edu.tw*

†Electronic supplementary information (ESI) available. See DOI: 10.1039/c6py01768a

Yang and co-workers[42] have observed similar textures in miktoarm star copolymers of the $PS(PI)_3$ type [where PS is polystyrene and PI is poly(isoprene)] but the architecture type was different when compared to star-block copolymers of the $(PS\text{-}b\text{-}PDMS)_3$ or $(SD)_3$ type.

Experimental

Materials

Benzene (Panreac, 99.8%) was purified *via* distillation from CaH_2 (Sigma-Aldrich, 95%) and was stored under high vacuum in a glass cylinder equipped with a stopcock, containing polystyrylithium oligomers ($PS^{(-)}Li^{(+)}$), exhibiting the characteristic orange-yellow color indicating the high purity level of benzene and the absence of air. Tetrahydrofuran (THF) (Fisher Scientific, 99.99%) was refluxed from metallic sodium spheres, and then distilled through CaH_2 in an Na/K alloy (3 : 1) under high vacuum. Hexamethylcyclotrisiloxane (D_3) (Acros Organics, 98%) was put in a flask, diluted with an equal volume of purified benzene, and stirred over CaH_2. The solvent was distilled and the monomer was sublimed into a flask containing $PS^{(-)}Li^{(+)}$ through short path distillation apparatus, where the solution was stirred for approximately 2 h at room temperature. Depending on the stability of the formed solution color, this step was repeated as many times as necessary in order for the color to remain constant. The solution was distilled (benzene) and sublimed (D_3) and finally stored in pre-calibrated ampoules followed by titration *via* the synthesis of a homopolymer poly(dimethylsiloxane). Styrene (Acros Organics, 99%) was purified by distillation from CaH_2 to dibutylmagnesium (Sigma-Aldrich, 1 M solution in heptane) and then stored in pre-calibrated ampoules. sec-BuLi (Sigma-Aldrich, 1.4 M in cyclohexane) was diluted in purified benzene, in a specific glass apparatus, under high vacuum. Trimethylchlorosilane (Sigma-Aldrich, 99+%) was purified under high vacuum through distillation from CaH_2 into pre-calibrated ampoules. Purification of the remaining reactants, linking agents dichlorodimethylsilane [$(CH_3)_2SiCl_2$] (Sigma-Aldrich, 99+%), trichloromethylsilane (CH_3SiCl_3) (Sigma-Aldrich, 99+%) and tetrachlorosilane ($SiCl_4$) (Sigma-Aldrich, 99+%) was accomplished through distillation from CaH_2 and storage under high vacuum after several freeze-drying cycles. Methanol (Fluka 99%) was used without any further purification, but a small quantity of the antioxidant-stabilizer 2,6-di-*tert*-butyl-*p*-cresol (Sigma-Aldrich, 99+%) was added. Methanol was the non-solvent in order to precipitate the intermediate and final materials, as well as for terminating all sample aliquots received from the polymerization solution for molecular weight control.

Synthesis

The synthetic procedure used for the preparation of the diblock copolymer precursors was living anionic sequential polymerization bearing one-fold excess of the siloxane monomer (Scheme 1). The synthesis was also accomplished

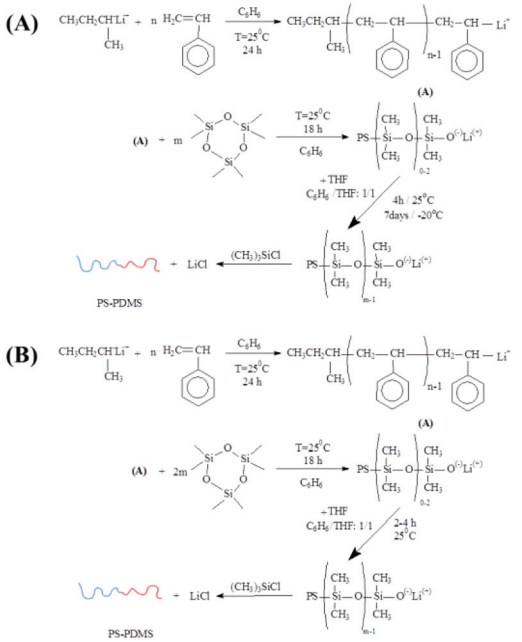

Scheme 1 Synthetic routes of: (A) PS-*b*-PDMS-*b*-PS triblock copolymer, (B) $(PS\text{-}b\text{-}PDMS)_3$ star-block copolymer and (C) $(PS\text{-}b\text{-}PDMS)_4$ star-block copolymer, using dichlorodimethylsilane, trichloromethylsilane and tetrachlorosilane as the linking agent respectively. Blue color corresponds to PS and red color to PDMS blocks.

successfully *via* a two-fold excess of the siloxane monomer. The living solution of $PS\text{-}b\text{-}PDMS^{(-)}Li^{(+)}$ was separated into three different glass apparatuses (Scheme 2). With the use of three different silane coupling agents [dichlorodimethylsilane ([$(CH_3)_2SiCl_2$]), trichloromethylsilane (CH_3SiCl_3) and tetrachlorosilane ($SiCl_4$)], the final star-block copolymers were synthesized. It is important to mention that the progress of all reactions was monitored by size exclusion chromatography

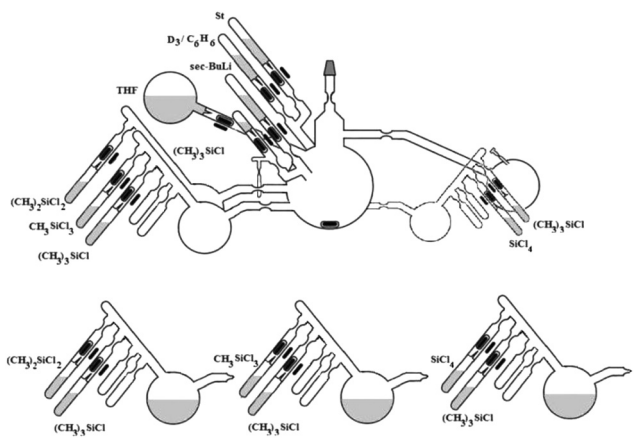

Scheme 2 Main glass reactor used for the synthesis of the diblock copolymer (PS-*b*-PDMS) under high vacuum (upper image) and the three sub-reactors (lower image) for the living polymer coupling by relevant chlorosilane reagents.

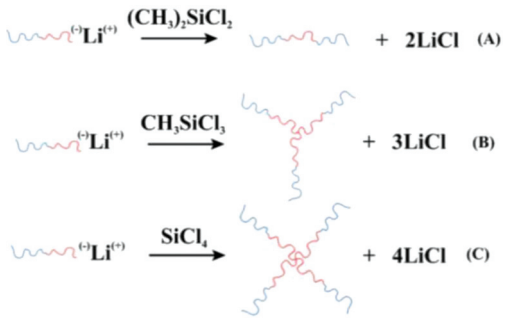

Scheme 3 Synthetic routes of: (A) PS-*b*-PDMS-*b*-PS triblock copolymer, (B) $(PS\text{-}b\text{-}PDMS)_3$ star-block copolymer and (C) $(PS\text{-}b\text{-}PDMS)_4$ star-block copolymer, using dichlorodimethylsilane, trichloromethylsilane and tetrachlorosilane as the linking agent respectively. Blue color corresponds to PS and red color to PDMS blocks.

(SEC) during the synthesis and the coupling reaction. In Scheme 3, the three different linking reactions are shown.

In detail, the synthesis of the diblock copolymers was accomplished by two different approaches, the "one" and "two" fold excess addition of the hexamethylcyclotrisiloxane (D_3) monomer. Following the first procedure[43] the final product is obtained after 10 days. However, the second method, which was reported in a previous study,[44] leads to the synthesis of the diblock copolymers within only 3 days. The reactions of both synthesis procedures are shown in Scheme 1.

A typical synthesis for the series of block copolymers SD-1, $(SD\text{-}1)_2$, $(SD\text{-}1)_3$ and $(SD\text{-}1)_4$ is given below. The first block (PS) was synthesized using 14.2 g (0.136 mol) styrene (first monomer) and 1.246 mmol secondary butyllithium (s-BuLi) in 250 ml of benzene (solvent). The polymerization was completed after 12–18 hours and a small aliquot of the solution was subsequently taken for molecular characterization, in order to determine the number average molecular weight for PS (11 400 g mol^{-1}). The next step was the addition of the second monomer, 17.8 g (0.080 mol) hexamethylcyclotrisiloxane (D_3), and due to the presence of polystyryl lithium living ends, the ring opening of D_3 was accomplished after approximately 18 hours. The addition of 250 ml of tetrahydrofuran (THF) was to create a polar environment in order to propagate the polymerization of D_3.

The ratio between the quantities of benzene and THF was approximately 1 : 1. After 4 hours the sample was placed in a constant temperature freezer (−20 °C) for one week. The number average molecular weight of the poly(dimethylsiloxane) block was estimated to be 14 350 g mol^{-1}. Subsequently, the solution was divided into three larger parts and one small aliquot of the precursor diblock was removed and terminated, again for molecular and also morphological characterization purposes.

The final and most time consuming step was the coupling and formation of the final triblock and star copolymers. The coupling agents used were dichlorodimethylsilane $(CH_3)_2SiCl_2$ (0.5607 mmol) for the $(SD\text{-}1)_2$ sample synthesis, trichloromethylsilane (CH_3SiCl_3) (0.3738 mmol) for the $(SD\text{-}1)_3$ sample and tetrachlorosilane ($SiCl_4$) (0.2804 mmol) for the sample $(SD)_4$. At intervals of 15, 30, 45 and 60 days small aliquots were removed from the solution for monitoring the progress of coupling *via* size exclusion chromatography. The results in all cases were not altered after 30 days which is a significant conclusion that can be made from the synthesis procedure. When the chromatography experiments showed that there was no alteration in molecular weight and/or in the ratio of the peaks, a small amount of trimethylchlorosilane $(CH_3)_3SiCl$ was added to the solution to deactivate any remaining uncoupled active sites. All samples were precipitated in methanol (containing the antioxidant additive 2,6-di-*tert*-butyl-*p*-cresol) which is a non-solvent for the synthesized polymers. The next step was oven vacuum drying and fractionation *via* a mixture of solvent and non-solvent (toluene/methanol respectively) at a constant temperature, in order to remove the undesired excess of the diblock copolymer.

The linear triblock copolymers and non-linear star-block copolymers were synthesized from the same diblock copolymer precursor (PS-*b*-PDMS). Scientific glass blowing was performed to create a specific and totally innovative glass apparatus for completing the anionically synthesized copolymers under high vacuum conditions (Scheme 2).

Characterization

Molecular characterization. For size exclusion chromatography measurements a PL-50 GPC system equipped with a pre-column, three PL gel columns and a refractive index detector was used, with THF as the eluent at a temperature of 35 °C. The system was calibrated with the PS-A and PS-B polystyrene standards from Polymers Laboratories. The flow rate of the eluent was 1 ml min^{-1}. Proton nuclear magnetic resonance (^{1}H-NMR) spectroscopy measurements were made in deuterated chloroform ($CDCl_3$) at room temperature, using a Bruker AC-250 spectrometer. Finally, a Gonotec 090 membrane osmometer was used for the number average molecular weight determination *via* membrane osmometry (MO). The measurements were performed at 35 °C with dried toluene as the solvent.

Thermal analysis. DSC experiments were carried out in a Perkin Elmer DSC 7 and also a Perkin Elmer DIAMOND DSC for studying the thermal behavior of PS-*b*-PDMS, PS-*b*-PDMS-*b*-PS and the star block copolymers. The samples were enclosed in aluminum caps and despite the fact that PDMS has a very low glass transition temperature, all samples undergo an initial heating process in order to erase the previous thermal/mechanical history of the samples. The collected data refer to the second heating procedure with a rate of 10 °C min^{-1}. The temperature range was −150 °C to 0 °C for the first instrument and 0 °C to 120 °C for the second instrument. Two different instruments were used, since the glass transition for the PS segment was barely observed due to the crystallization of the PDMS segment. For TGA, the specimens were placed in a thermogravimetric analyzer (Perkin Elmer Pyris 1 TGA) at room temperature, and then heated to 750 °C at a rate of 10 °C min^{-1}.

Morphological characterization. The morphological characterization of the synthesized polymers was accomplished *via* transmission electron microscopy (TEM) and small angle X-ray scattering (SAXS), which reveal well-ordered structures due to the self-assembly of these polymeric systems. In all cases the samples were ultra cryo-microtomed at temperatures well below the T_g of both segments in order to avoid interference with the structural properties. Thin sections from films obtained from 5 wt% cast-solutions of all samples in toluene were obtained by ultra-cryomicrotomy at a very low temperature (−160 °C) using a Reichert-Leica ultracut microtome.

Bright-field TEM images were obtained by mass-thickness contrast on a JEOL TEM-2100X transmission electron microscope operating at an accelerating voltage of 200 kV. No staining was necessary, since the intrinsic difference in the electron density of the PS and PDMS blocks provided adequate bright field contrast, leading to images with a characteristic black color for PDMS (increased mass contrast due to high electron density) and white for the segment of PS (decreased mass contrast due to lower electron density).

SAXS experiments were conducted at the synchrotron X-ray beam-line BL23A SWAXS end-station at the National Synchrotron Radiation Research Center (NSRRC) in Hsinchu Taiwan. The wavelength of the X-ray beam was 0.1033 nm. A MAR CCD X-ray detector (MAR USA) was used to collect the two-dimensional (2D) SAXS patterns, where the detector pixel size was 0.158 mm and the distance between the sample and the detector was 3093.150 mm. A one-dimensional (1D) linear profile was obtained through the integration of the 2D pattern. The beam center was at (512.1, 581.0) (X, Y) and the photon energy per sample was 12 keV.

Three-dimensional electron tomography was used to more efficiently examine in great detail the chevron structure observed in the case of sample $(SD\text{-}1)_3$, a three arm star block copolymer. In this case, the output was a video file produced by the 3D reconstruction of 181 TEM images, obtained under the same specification and magnification from the same polymeric film region, by altering only the x-axis angle (tilting on the TEM 3D holder) by one degree per image.

Results and discussion

The molecular, thermal and morphological characteristics of the linear and complex architecture copolymers are summarized in Table 1. It should be noted that the four arm star-block copolymer $[(SD\text{-}3)_4]$ presented in this work was synthesized from a diblock copolymer precursor (SD-3) with slightly different molecular characteristics when compared with samples derived from precursor SD-1. In total three diblock copolymers (SD-1, SD-2 and SD-3), one triblock copolymer $[(SD\text{-}1)_2]$, two three arm star-block copolymers $[(SD\text{-}1)_3$ and $(SD\text{-}2)_3]$ and one four-arm star block copolymer $[(SD\text{-}3)_4]$ were synthesized.

Molecular characterization

The PS homopolymers, the intermediate diblock arms and the final linear (triblock) and non-linear (star block) copolymers were characterized *via* size exclusion chromatography (SEC), proton nuclear magnetic resonance spectroscopy (^{1}H-NMR) and membrane osmometry (MO) to verify the molecular characteristics. Narrow molecular weight distribution and compositional and molecular homogeneity for the final copolymers were concluded. In Fig. S1a and b of the ESI† the data from GPC and ^{1}H-NMR are given for representative samples. The molecular characteristics of the samples are summarized in Table 1.

In order to purify the synthesized copolymers from the unreacted excess of the diblock arm, mass fractionation in a mixture of a good solvent (toluene)/non-solvent (methanol) was performed. No homopolymer or other byproducts were observed in the final complex architecture materials as is evident from the SEC chromatograms (Fig. S1a†). ^{1}H-NMR experiments confirmed the successful synthesis since chemical resonances at 6.7–7.5 ppm and at 0.1–0.3 ppm are evident due to the 5 aromatic protons of the aromatic group of the styrene monomeric unit and the 6 methyl protons of the siloxane monomeric unit, respectively (Fig. S1b†).

Thermal analysis

Differential scanning calorimetry (DSC) and thermogravimetric analysis (TGA) experiments were carried out to

Table 1 Molecular, thermal and morphological characteristics of the linear and complex architecture copolymers (S corresponds to PS and D to PDMS)

Sample	$\bar{M}_n^{PS}$ [a] (g mol^{-1})	$\bar{M}_n^{PDMS}$ [a] (g mol^{-1})	$\bar{M}_n^{total}$ [b] (g mol^{-1})	$Đ_M$ [c]	T_g^{PS} (^{o}C)	T_g^{PDMS} (^{o}C)	f_{PDMS} [d] (wt%)	Morphology[e]	d[f] (nm)
SD-1	11 400	14 350	25 750	1.04	90	−125	0.58	L	30.7
SD-2	19 900	12 550	32 450	1.05	90	−125	0.41	HC	29.4
SD-3	9400	10 200	19 600	1.04	88	−125	0.54	L	25.0
$(SD\text{-}1)_2$	22 800	28 700	51 500	1.06	89	−129	0.58	L	30.2
$(SD\text{-}1)_3$	34 200	43 050	77 250	1.07	92	−127	0.58	L	30.2
$(SD\text{-}2)_3$	59 700	37 650	97 350	1.08	89	−129	0.41	HC	32.6
$(SD\text{-}3)_4$	37 600	40 800	78 400	1.07	89	−125	0.54	L	22.5

[a] Number average molecular weight of the PS and the PDMS blocks from SEC and MO. [b] Total number average molecular weight of the copolymers from SEC and MO. [c] Polydispersity index as given by SEC. [d] PDMS volume fraction calculated from the mass fraction as obtained from ^{1}H-NMR (d_{PS} = 1.060 g mol^{-1}, d_{PDMS} = 0.930 g mol^{-1}). [e] Verified from SAXS and TEM studies (HC: hexagonally packed cylindrical morphology; L: lamellar morphology). [f] d-Spacing calculated from the first permitted peak q value (nm^{-1}) in the SAXS plots through the Bragg's law equation.

study the thermal properties of the synthesized materials. In Fig. S2 of the ESI† the DSC and TGA thermographs of the 3-arm star block copolymer sample $(SD\text{-}1)_3$ are shown. The glass transition temperatures of the PS (T_g^{PS}) and PDMS (T_g^{PDMS}) were approximately 90 °C and −125 °C, respectively. Meanwhile, the crystallization temperature (T_c) of PDMS blocks could not be observed in all cases (especially, in the complex architecture star copolymers). The absence of the crystallization temperature (T_c) of PDMS during the DSC measurements is attributed to the fact that PDMS forms the core of the material and it is difficult to crystallize whereas the outer PS chains are in the glassy state. From TGA experiments, the degradation temperature (T_d) is estimated to be approximately 390 °C for the complex architecture copolymers and 320 °C for the corresponding diblocks exhibiting a unique increased thermal stability for the more complex samples.

Morphological characterization

The as-cast bulk samples were dried in a vacuum oven for three days at 120 °C to remove the residual solvent followed by thermal annealing at 180 °C for 12 hours, and then rapid quenching was performed using liquid nitrogen for TEM and SAXS experiments. For the linear diblock copolymer SD-1 (as abbreviated in Table 1), alternating bright and dark layers can be clearly observed in the TEM images (Fig. 1A), suggesting the formation of a lamellar phase. The corresponding one-dimensional (1D) SAXS profile shows the reflection peaks at relative q values of 1 : 2 : 3 : 4, further confirming the formation of a lamellar phase (Fig. 1B). By increasing the arm number to two [sample $(SD\text{-}1)_2$], the TEM image and SAXS profile (Fig. 1C and D) exhibit similar morphologies. When the arm number is further increased [n = 3, sample $(SD\text{-}1)_3$], an interesting zig-zag pattern can be clearly identified in the TEM image (Fig. 1E). Additional TEM analysis with higher magnification was carried out for sample $(SD\text{-}1)_3$ and it is included in the ESI.† As shown in Fig. S3,† there are no cracks or indication of stretching at the grain boundaries of the lamella regions. Three-dimensional electron tomography was also carried out to examine the observed chevron structure in detail (Fig. 2). The 3D electron tomography result suggests that the specific structure is a uniform texture within the mass of the thin film as indicated by the rotating movie uploaded in the ESI.† Interestingly, by further increasing the arm number to four [n = 4, $(SD\text{-}3)_4$], there is no formation of such a chevron structure. Instead, the TEM and SAXS results of the $(SD\text{-}3)_4$ (Fig. 1G and H) only show an ordinary lamellar pattern with alternating bright and dark layers and the scattering results give the relative q values of 1 : 2 : 3 : 4 as expected for such a morphology. This reconstruction leads to images showing this chevron like morphology for this nonlinear block copolymer. The

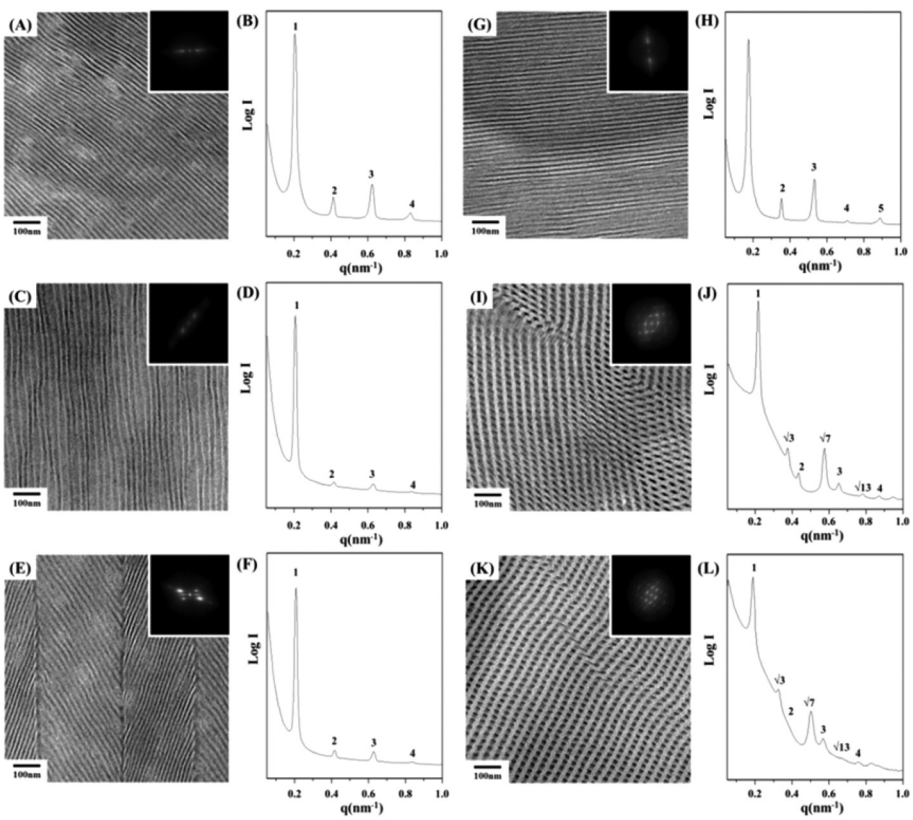

Fig. 1 TEM micrographs and the corresponding 1D SAXS profiles of the linear diblock copolymer SD-1 (A, B), two-arm ABA triblock copolymer, $(SD\text{-}1)_2$ (C, D), three-arm star-block copolymer, $(SD\text{-}1)_3$ (E, F), four-arm star-block copolymer, $(SD\text{-}3)_4$ (G, H), linear diblock copolymer SD-2 (I, J) and three-arm star-block copolymer, $(SD\text{-}2)_3$ (K, L).

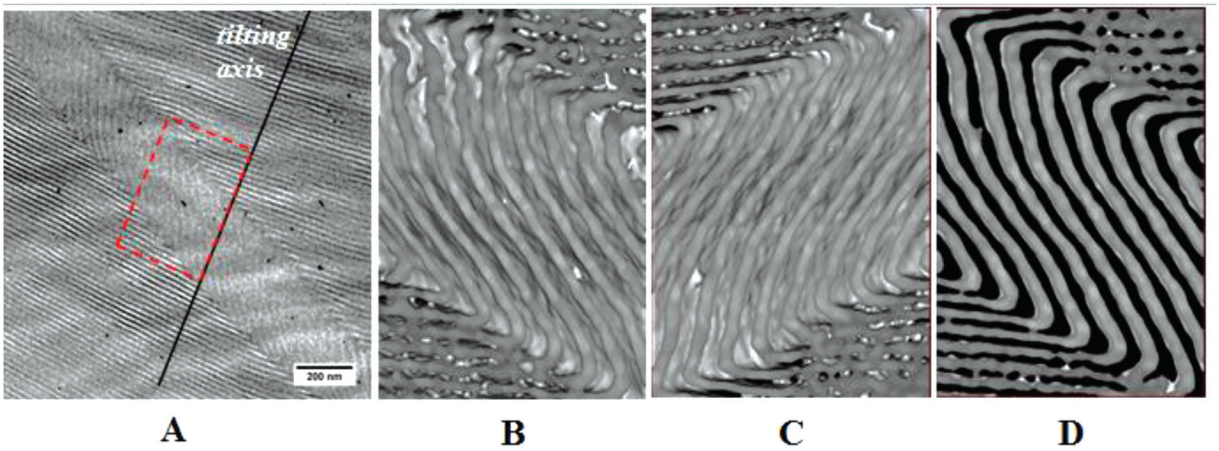

Fig. 2 TEM tomography on the $(SD)_3$-1 star block copolymer. (A) Area of tilting, (B): −60° tilting, (C): +60° tilting, and (D) "zoom in" at 90°.

reconstruction has only a few structural defects thus the observation of the aforementioned structure is clear. In Fig. 2 the 3D reconstruction for the 0° tilting TEM image (with the tilting area marked), the tilting axis, and three snapshots of the produced video file at −60°, +60° and the zoom in at 90° are given.

To further study the architecture effect on the self-assembled morphologies of such $(PS\text{-}b\text{-}PDMS)_n$ type star-block copolymers, cylinder-structured PS-*b*-PDMS samples [diblock copolymer (SD-2) and a three-arm star-block copolymer $(SD\text{-}2)_3$] were examined by TEM and SAXS in order to be compared with the lamella-structured linear and non-linear PS-*b*-PDMS samples. As shown in Fig. 1I and K, similar images of dark elliptical PDMS microdomains hexagonally packed in the PS matrix are evident for both samples [(SD-2) and $(SD\text{-}2)_3$]. It should be noted that the elliptical texture of PDMS microdomains under TEM might be attributed to the deformation of the cylindrical microdomains caused by the solution-cast process.[26] The grey stripes connecting the PDMS microdomains are attributed to the oblique projection of the cylinder axis. The corresponding 1D SAXS profiles (Fig. 1J and L) of both samples show the same reflection peaks at relative q values of $1:\sqrt{3}:\sqrt{4}:\sqrt{7}:\sqrt{9}:\sqrt{13}$, further confirming the formation of hexagonally packed cylindrical phases. Consequently, on the basis of the morphological observations and scattering results, both (SD-2) and $(SD\text{-}2)_3$ samples exhibit ordinary cylinder morphologies with hexagonal packing in bulk. There is no significant difference between the linear diblock copolymer and the three-arm star block copolymer on the obtained morphology as in the previous case. These results indicate that the three-arm architecture of the copolymers does not amend the self-assembled morphologies of the cylinder-structured system. Therefore, the origin of the formed chevron texture may be attributed to the asymmetry of the geometric repeating unit for the three-arm architecture, and only appears in the three-arm lamella-structured star-block copolymer.

It is noted that the dependence of the *d*-spacing determined by using the primary peak of the SAXS reflections on the architecture in both sets (SD-1) *versus* $(SD\text{-}1)_3$ and (SD-2) *versus* $(SD\text{-}2)_3$ of the copolymers is insignificant even though there is a substantial increase in the total molecular weight. On the basis of the three-arm architecture and the determined spacing of the self-assembled textures, two conformations for the PDMS chains are proposed (Fig. 3B and D) in comparison with that of the linear diblock copolymer (Fig. 3A). These two models are illustrated based on the ability of the PDMS chains to create loops or bridges in accordance with the corresponding architectures. Under both conditions, the *d*-spacings of the self-assembled morphologies are approximately a two-time repetition of the PS and PDMS chains as the linear diblock copolymer instead of the interdigitated mode.

Specifically, the star architecture will not alter drastically the *d*-spacing of the self-assembled morphology. The conformation of the star architecture evidently leads to a different conformational entropy. In the case of loop conformations (Fig. 3B), looping of the middle-block (PDMS) at the interface will lead to an entropic penalty. Meanwhile, the strong segregation strength of the PS-*b*-PDMS system will lead to the stretch of both PS and PDMS block chains along the intermediate dividing surface (IMDS) and therefore the average nearest-neighbor distance between the chemical junctions will be simultaneously reduced. Consequently, looping of the PDMS chain will not only lead to an entropic penalty but also prohibit the stretching of PS and PDMS block chains. By contrast, the formation of the PDMS bridges (Fig. 3C) will give rise to a Gibbs free energy favored state for the PS-*b*-PDMS star-block copolymer system. Based on our recent reported work, the entropic effect due to the topology of the star-block copolymers will lead to the formation of bridge conformations.[26] Once a star-block copolymer possesses a higher number of chain ends a higher entropic penalty in the parallel orientation will be created. As a result, with the increase in the arm number, the entropic effect due to the star architecture will overcome the enthalpic interactions at the interface, in particular from the substrate, resulting in the spontaneous formation of perpendicularly oriented lamellae or cylinders. On the basis of the proposed bridge conformation and due to the

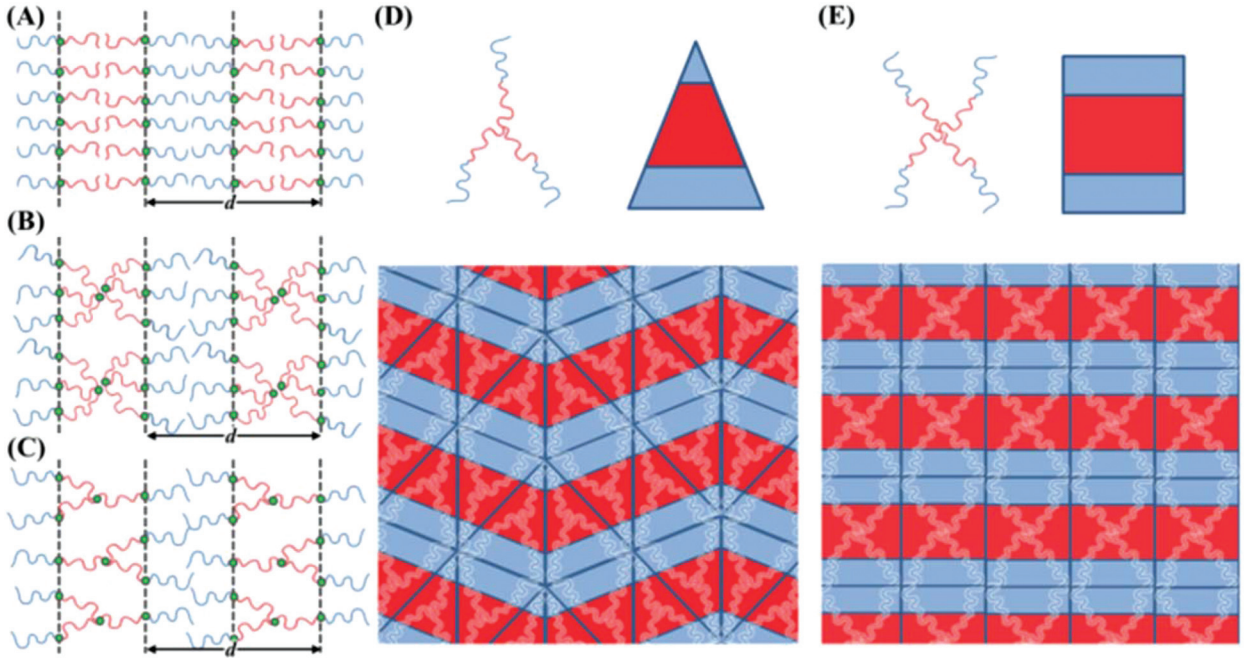

Fig. 3 Schematic illustration of the models of polymer chain packing. Polystyrene and poly(dimethylsiloxane) blocks are shown in red and blue colour, respectively. (A) shows the polymer chain model of the linear diblock copolymer. (B) and (C) correspond to two different conformations based on the ability of the PDMS chains to create loops or bridges for the three-arm architecture. (D) and (E) show the packing of the geometric unit for the three-arm and four-arm architecture, respectively.

overcrowding effect of the star-block copolymer, the formation of chevron topology with the three-arm architecture can be explained by the molecular chain model as illustrated in Fig. 3D. The molecular architecture of the three-arm and four-arm star-block copolymers can be regarded as triangle (Fig. 3D) and square (Fig. 3E) geometric repeating domains, respectively. In order to achieve the state with lower packing energy from self-assembly, it is necessary to form a closely packed texture from the building units into a well-ordered lamellar structure. For the three-arm architecture, the triangle unit can be assembled into two different directions (up and down). Once the triangle domains are packed along different directions, it will create an interesting V-shape grain boundary. Consequently, with the repeating of the V-shape grain boundary, the chevron patterns are formed (Fig. 2D). On the other hand, for the four-arm architecture, the square domain is symmetric in both directions (up and down), leading to a packing of only one simple lamellar structure without any special grain boundary (Fig. 2E). In the case of the cylinder-structured system, the relative domains will pack along the normal direction to form a well-ordered cylinder structure (Fig. S4†) without forming any special structures. Complex structures such as the ones exhibited by the star block copolymers in this study have potential for a variety of applications and especially as thin films in nanotechnology since controlled orientation is feasible, and therefore may minimize further the molecular weight limits towards nanotechnology applications and directed self-assembly features as already reported in previous studies for PS-*b*-PDMS diblock copolymers.[6,26,44–48]

Conclusions

In summary, this work presents a study on the self-assembly of (PS-*b*-PDMS)$_{n=1,\ 2,\ 3,\ 4}$ block copolymers of various architectures (linear and non-linear), which were synthesized through anionic polymerization in combination with chlorosilane linking chemistry. It was possible to synthesize well-defined star block copolymers with the core consisting of polydimethylsiloxane. To the best of our knowledge in the literature no references on the synthesis of such star block copolymers are reported. Additionally, it was found that the self-assembly of these systems depends upon their architectures due to the need for minimum total free energy in order to maintain at equilibrium their structure without any entropy constraints. The chevron texture was verified for a lamella-structured three arm star-block copolymer. Exploitation of the architecture effect on the self-assembly of block copolymers is very appealing in a wide variety of applications, in particular nanopatterning technologies for block copolymer lithography.

Acknowledgements

P. G. and A. A. would like to acknowledge financial support through the European Union Seventh Framework Program (FP7/2007–2013), as part of the LAMAND Project (grant agreement no. 245565). T. Y. Lo and R. M. Ho would like to thank the National Science Council of the Republic of China, Taiwan, for financially supporting this research under grant MOST 105-

2633-M-007-003 from NSC no. 101-2221-E-007-038-MY3. Also the Network of Research Supporting Laboratories at the University of Ioannina for ^{1}H-NMR experiments and the National Synchrotron Radiation Research Center (NSRRC) in Hsinchu City, Taiwan for the SAXS experiments are acknowledged.

References

1 F. S. Bates and G. H. Fredrickson, *Phys. Today*, 1999, **52**, 32.
2 F. S. Bates, M. A. Hillmyer, T. P. Lodge, C. M. Bates, K. T. Delaney and G. H. Fredrickson, *Science*, 2012, **336**, 434–440.
3 J. C. Saam and F. G. Fearon, *Ind. Eng. Chem. Prod. Res. Dev.*, 1971, **10**, 10–14.
4 J. C. Saam, D. J. Gordon and S. Lindsey, *Macromolecules*, 1970, **3**, 1–4.
5 T.-Y. Lo, C.-C. Chao, R.-M. Ho, P. Georgopanos, A. Avgeropoulos and E. L. Thomas, *Macromolecules*, 2013, **46**, 7513–7524.
6 C.-C. Chao, R.-M. Ho, P. Georgopanos, A. Avgeropoulos and E. L. Thomas, *Soft Matter*, 2010, **6**, 3582–3587.
7 U. Breiner, U. Krappe and R. Stadler, *Macromol. Rapid Commun.*, 1996, **17**, 567–575.
8 U. Breiner, U. Krappe, V. Abetz and R. Stadler, *Macromol. Chem. Phys.*, 1997, **198**, 1051–1083.
9 U. Breiner, U. Krappe, T. Jakob, V. Abetz and R. Stadler, *Polym. Bull.*, 1998, **40**, 219–226.
10 U. Breiner, U. Krappe, E. L. Thomas and R. Stadler, *Macromolecules*, 1998, **31**, 135–141.
11 A. Avgeropoulos, B. J. Dair, N. Hadjichristidis and E. L. Thomas, *Macromolecules*, 1997, **30**, 5634–5642.
12 A. Avgeropoulos and N. Hadjichristidis, *J. Polym. Sci., Part A: Polym. Chem.*, 1997, **35**, 813–816.
13 N. Hadjichristidis, *J. Polym. Sci., Part A: Polym. Chem.*, 1999, **37**, 857–871.
14 N. Hadjichristidis and A. Hirao, *Anionic Polymerization: Principles, Practice, Strength, Consequences and Applications*, Springer, 2015.
15 N. Hadjichristidis, M. Pitsikalis, S. Pispas and H. Iatrou, *Chem. Rev.*, 2001, **101**, 3747–3792.
16 Y. Huang, L. Bu, D. Zhang, S. Chengwei, Z. Xu, L. Bu and J. W. Mays, *Polym. Bull.*, 2000, **44**, 301–307.
17 G. Mountrichas, M. Mpiri and S. Pispas, *Macromolecules*, 2005, **38**, 940–947.
18 L.-K. Bi and L. J. Fetters, *Macromolecules*, 1976, **9**, 732–742.
19 K. Hong, Y. Wan and J. W. Mays, *Macromolecules*, 2001, **34**, 2482–2487.
20 P. H. Nelson, G. C. Rutledge and T. A. Hatton, *Comput. Theor. Polym. Sci.*, 1998, **8**, 31–38.
21 M. Matsen, *J. Chem. Phys.*, 1998, **108**, 785–796.
22 M. Matsen and F. Bates, *Macromolecules*, 1996, **29**, 1091–1098.
23 M. W. Matsen and M. Schick, *Macromolecules*, 1994, **27**, 187–192.
24 W. Shi, A. L. Hamilton, K. T. Delaney, G. H. Fredrickson, E. J. Kramer, C. Ntaras, A. Avgeropoulos, N. A. Lynd, Q. Demassieux and C. Creton, *Macromolecules*, 2015, **48**, 5378–5384.
25 W. Shi, N. A. Lynd, D. Montarnal, Y. Luo, G. H. Fredrickson, E. J. Kramer, C. Ntaras, A. Avgeropoulos and A. Hexemer, *Macromolecules*, 2014, **47**, 2037–2043.
26 T.-Y. Lo, A. Dehghan, P. Georgopanos, A. Avgeropoulos, A.-C. Shi and R.-M. Ho, *Macromolecules*, 2016, **49**, 624–633.
27 C. Tsitsilianis, D. Papanagopoulos and P. Lutz, *Polymer*, 1995, **36**, 3745–3752.
28 Y. Zhu, S. P. Gido, M. Moshakou, H. Iatrou, N. Hadjichristidis, S. Park and T. Chang, *Macromolecules*, 2003, **36**, 5719–5724.
29 H. Gao and K. Matyjaszewski, *Macromolecules*, 2008, **41**, 1118–1125.
30 H. Gao and K. Matyjaszewski, *J. Am. Chem. Soc.*, 2007, **129**, 11828–11834.
31 H. Gao and K. Matyjaszewski, *Macromolecules*, 2006, **39**, 4960–4965.
32 H. Gao, K. Min and K. Matyjaszewski, *Macromol. Chem. Phys.*, 2007, **208**, 1370–1378.
33 G. Polymeropoulos, D. Moschovas, A. Kati, A. Karanastasis, S. Pelekanou, P. Christakopoulos, G. Sakellariou and A. Avgeropoulos, *J. Polym. Sci., Part A: Polym. Chem.*, 2015, **53**, 23–32.
34 J. Chen, E. Thomas, C. Ober and G.-P. Mao, *Science*, 1996, **273**, 343–346.
35 M. Krumova, S. Henning and G. H. Michler, *Philos. Mag.*, 2006, **86**, 1689–1712.
36 Y. Mori, L. S. Lim and F. S. Bates, *Macromolecules*, 2003, **36**, 9879–9888.
37 C. C. Honeker and E. L. Thomas, *Chem. Mater.*, 1996, **8**, 1702–1714.
38 Y.-H. Ha and E. L. Thomas, *Macromolecules*, 2002, **35**, 4419–4428.
39 M. Matsen, *J. Chem. Phys.*, 1997, **107**, 8110–8119.
40 S. P. Gido and E. L. Thomas, *Macromolecules*, 1994, **27**, 6137–6144.
41 E. Burgaz and S. P. Gido, *Macromolecules*, 2000, **33**, 8739–8745.
42 L. Yang, S. Hong, S. P. Gido, G. Velis and N. Hadjichristidis, *Macromolecules*, 2001, **34**, 9069–9073.
43 V. Bellas, H. Iatrou and N. Hadjichristidis, *Macromolecules*, 2000, **33**, 6993–6997.
44 C.-C. Chao, T.-C. Wang, R.-M. Ho, P. Georgopanos, A. Avgeropoulos and E. L. Thomas, *ACS Nano*, 2010, **4**, 2088–2094.
45 N. Politakos, E. Ntoukas, A. Avgeropoulos, V. Krikorian, B. D. Pate, E. L. Thomas and R. M. Hill, *J. Polym. Sci., Part B: Polym. Phys.*, 2009, **47**, 2419–2427.
46 W. Bai, A. F. Hannon, K. W. Gotrik, H.-K. Choi, K. Aissou, G. Liontos, K. Ntetsikas, A. Alexander-Katz, A. Avgeropoulos and C. A. Ross, *Macromolecules*, 2014, **47**, 6000–6008.
47 K.-H. Tu, W. Bai, G. Liontos, K. Ntetsikas, A. Avgeropoulos and C. A. Ross, *Nanotechnology*, 2015, **26**, 375301.
48 K. Lee, M. Kreider, W. Bai, L.-C. Cheng, S. Safari Dinachali, K.-H. Tu, T. Huang, K. Ntetsikas, G. Liontos, A. Avgeropoulos and C. A. Ross, *Nanotechnology*, 2016, **27**, 465301.

